ON HIGH-TEMPERATURE CREEP OF CONCRETE

H. GROSS*

Imperial College of Science and Technology, London, United Kingdom

(at present: Siempelkamp Giesserei K.G., D-415 Krefeld, Germany)*

SUMMARY

With the fast development of prestressed concrete pressure vessels for nuclear power stations and the growing concern about the safety of building structures against fire hazards, interest has increased in the knowledge of the behaviour of concrete at elevated and high temperatures and its effects on the strain history of loaded structures.

Since complex configurations of structures render the partial differential equations of the stress analysis problem insoluble in closed form, techniques for numerical analyses suitable for computer programming are required.

The change in the structures' stiffness matrix due to ambient or thermal creep effects is accounted for by the employment of thermal relaxation weighting factors which are arrived at in a rigorous mathematical procedure and valued on the basis of data obtained from experiments performed for thermal creep compliance.

The contents of the paper presented may be described as follows.

The quest for data on thermal creep compliance is set forth. The creep curves obtained are drawn. Linearity in the stress-dependence of the initial thermal strains is observed for low and moderately high temperatures. A formula for the determination of thermoelastic strains is proposed. Values for the ultimate initial and the ultimate creep strains are arrived at. The bandwidth between the domains of safe and failure-procuring test conditions is drawn.

A formula is proposed for the reduction of the modulus of elasticity with temperature. Formulae of tri-linear nature are designed for the temperature-dependence of the ultimate stress/cold strength ratio and for the dependence of the ultimate test temperature on the stress/cold strength ratio. The modulus of quasi-thermoelasto-plasticity is introduced. A formula is devised for the temperature-dependence of the ultimate cylinder strength.

The applicability of the superposition hypothesis to the overlay of thermal creep strains is proven.

The quasi-linearity of the creep rate—time relation in the double logarithmic scale is recognized. A mathematical equation is proposed to fit thermal creep curves. Experimentally substantiated expressions for the temperature and stress-dependence of the pertaining parameters are given.

Formulae are proposed for the development of thermal creep strains and thermoviscoelastic strains. The author's general formula for the determination of linear thermoviscoelastic strains occurring in virgin concrete is arrived at.

Using the proposed subprogram CRELAX, normalized thermal creep curves are first transformed to thermal relaxation curves; subsequently, the author's thermal relaxation weighting factors are evaluated.

1. INTRODUCTION

Axisymmetric or spherical concrete structures designed with tensioned or non-tensioned steel reinforcement are used in civil engineering practice as reactor pressure vessels, containers for chemicals, water towers or reservoirs, submarine oil tanks, caissons, bunkers, air-raid shelters, silos, cupolas, lighthouses, industrial chimneys and television aerial masts.

In the course of analysing such structures using finite element and finite difference computing techniques [1], the author investigated the behaviour of concrete at ambient, elevated and high temperatures, and subsequently studied its effects on the structures' strain history. Since stress analysis problems of continua are insoluble in closed form, the strain history is reproduced matrix-theoretically by defining sets of scalar thermal relaxation factors which act as multipliers of the coefficients of the structures' stiffness matrix as present in the global force-deformation equation.

2. EXPERIMENTAL INVESTIGATION

2.1. RECORDED CREEP STRAINS

Except for the residual strength of concrete cylinders after heat testing, the data reported were obtained from experiments conducted on the creep testing machines designed by the author [1,2].

Having established a uniform temperature distribution throughout the cylinders by preheating them for one day at the relevant temperatures, a fixed compressive load equivalent to a stress / cold strength ratio of $s = 0.2$, 0.4 or 0.66 was applied. All cylinders were of the same mix, of the size $\varnothing$ 60 x 180 mm and between six and twelve months old when tested. Their compressive cold strength worked out at $c'_{yu} = 42\ N/mm^2$.

The basic information acquired is at hand in form of creep curves displayed in figs. (1) to (5), the parameter being the test temperature.

2.2. THERMOELASTIC STRAINS

A parameter study is carried out on fig. (6) to show the effect of the stress / cold strength ratio on the formation of thermoeleastic strains. Scaling all readings as if they were taken at $s = 0.2$, a normalized profile common to the results obtained for the three different ratios s may be drawn, as done in fig. (7).

Independent of the load level, a local peak in the strains is registered at 60 °C. The fitting of a single, monotonically increasing function to the test data is thus precluded, leaving as the simplest solution the superposition of a tri-linear function

$$\varepsilon_{0.2}(T) = \varepsilon_{0.2}(20\ ^\circ C) \cdot f(T) \qquad (1)$$

$$f(T) = \begin{cases} (1.0 + 0.00833\ (T - 30)) & (30 \leq T \leq 60) \\ (1.25 - 0.00250\ (T - 60)) & (60 \leq T \leq 110) \\ (1.125 + 0.00349\ (T - 110)) & (110 \leq T \leq 350) \end{cases}$$

where $\varepsilon_{0.2}$ (20 °C) = 320 μ and the term ambient is applicable to temperatures up to 30 °C.

Analysing fig. (8), the following approximate field function may be described for temperatures equal to or higher than 200 °C

$$\varepsilon\ (s,T,0) = \left(\frac{s}{0.1}\right)^{1\ +\ e\ (s,T)} \left(\varepsilon_{0.1}\ (200\ ^{\circ}C) + 15.4\ (0.01\ T - 2)^4\right) \quad (\text{in } \mu) \qquad (2)$$

where $e\ (s,T) = 1.5\ \left(\frac{s}{0.1} - 1\right)\ (0.001\ T - 0.18)$

for s = 0.1, the exponent e (s,T) becomes zero, rendering the solution of eq. (2) thermoelastic.

$\varepsilon_{0.1}$ (200 °C), which amounts to 210 μ, and the strains for T ≧ 200 °C may be determined using formula (1).

2.3. ULTIMATE THERMAL STRAINS

Fig. (6) infers that within the range tested, concrete of the given mix and age fails under loads imposing strains greater than about 0.4%. By tentative extrapolation along the confidence limits drawn from experiments in fig. (9), however, for s = 0.1 and T = 600 °C a thermoelasto-plastic strain of about 1% may be predicted. This value presumably coincides with the maximum ultimate thermoelasto-plastic deformation, as concrete ceases to take any significant stress when heated to temperatures beyond 600 °C. Cf. with figs. (12), (14), (15). Tentatively, thus

$$\varepsilon(T,t = 0)_{max.} \cong 1\% \qquad (3)$$

As regards ultimate creep strains, fig. (10) indicates that within the domain 0.2 ≧ s ≧ 0.66, the 7-day creep strains do not exceed values of about 1%, irrespective of the test temperature. Since by extrapolation along the creep profiles in figs. (1) to (5) the estimated maximum increase in strain beyond seven days is limited to about 20%, the ultimate total creep strain may be expected to settle at

$$\varepsilon(T,t = \infty)_{max.} \cong 1.2\% \qquad (4)$$

2.4. THERMALLY INDUCED SHRINKAGE STRAINS

The local maximum in the strain developments at about 60 °C indicates the presence of drying shrinkage. The thermally induced shrinkage strains recorded are entered in fig. (11). Outside the extension of the local peak, i.e. for 110 and 140 °C, no significant shrinkage strains were detected. For temperatures of 60 and 80 °C, however, finite strain readings of 180 and 160 μ were taken at the end of the seventh day after preheating.

3. PHYSICAL REPRESENTATION

3.1. CONSTITUTIVE RELATIONSHIPS

The temperature-dependent stress-strain curves obtained during load application are drawn in fig. (12), showing linearity of the strains in the stress variable up to about 200 °C.

With the environmental condition becoming more severe, a transition to thermoplastic behaviour takes place, and for temperatures beyond 350 °C, concrete quickly deteriorates.

3.2. MODULUS OF THERMOELASTO-PLASTICITY

Once the initial thermoelastic strains are recorded, the modulus of thermoelasto-plasticity is determined by dividing the stress by the strain. For a stress / cold strength ratio of s = 0.2, errors in the initial strain readings due to viscous effects are reduced, since in the corresponding test procedures the load was applied within 20 sec.

Save in the vicinity of 60 °C, where the associated value drops to 80 % of the initial one, an inversed quadratic parabola may be fitted to the test results entered in fig. (13)

$$m_{0.2} = 4.81\ (452 - T)^{1/2} \qquad (\text{in } \%) \qquad (5)$$

where $m_{0.2}$ is defined by $E_{ini}\ (T) / E_{ini}\ (20\ ^{\circ}C)$

3.3. ULTIMATE STRESS / COLD STRENGTH RATIO

The limiting ratios are plotted against the test temperature in fig. (14). Since the load is applied by weights of finite magnitudes, only upper and lower bound solutions can be produced. Upper bound values symbolize the collapse of the specimens, while for lower bound values the corresponding load ist still endured. The limiting profile may be approximated by a tri-linear function

$$\begin{aligned} s_{ult}\ (T) &= 1.0 - 0.001\ (T - 20) && (20 \leq T \leq 350) \\ &= 0.66 - 0.00457\ (T - 350) && (350 \leq T \leq 452) \\ &= 0.2 - 0.000746\ (T - 452) && (452 \leq T \leq 700) \end{aligned} \qquad (6)$$

3.4. ULTIMATE TEMPERATURES

The higher temperatures endured may be expressed in terms of the stress / cold strength ratio by investing eqs. (6)

$$\begin{aligned} T_{ult}\ (s) &= 1000\ (1.0 - s) + 20 && (0.66 \leq s \leq 1) \\ &= 219\ (0.66 - s) + 350 && (0.2 \leq s \leq 0.66) \\ &= 1340\ (0.2 - s) + 452 && (0.02 \leq s \leq 0.2) \end{aligned} \qquad (7)$$

3.5. MODULUS OF QUASI-THERMOELASTO-PLASTICITY

A more general modulus of thermoelasto-plasticity which tolerates small viscous contributions to initial deformations may be defined. Relying on the experimentally corroborated values in figs. (13) and (14), the author suggests a formula of inverted parabolic nature

$$m_s = a\ (s)\ (T_{ult}\ (s) - T)^{1/2} \qquad (8)$$

where $T_{ult}\ (s)$ is given by eq. (7) and the parameter a (s) is obtained from the simple expression

$$a\ (s) = 100\ (T_{ult}\ (s) - 20\ )^{-1/2} \qquad (9)$$

Eq. (5) is identically satisfied. Based on formula (8), the temperature-induced deterioration of concrete can be predicted for various stress / cold strength ratios. Examples are shown in fig. (13) for $s = 0.1$ and 0.8.

3.6. ULTIMATE HOT STRENGTH

As revealed by the entries in fig. (15), the reduction in ultimate strength, determined after gently cooling and removal from the furnace, does not exceed 10% as long as the test temperature falls below 150 °C. For higher temperatures, the author found the simple linear relation

$$n_{7\text{-day}} = (120 - 0.171\ T) \qquad (150 \leq T \leq 700) \qquad (10)$$

where n is defined by the ratio $c'_{yu}\ (T)\ /\ c'_{yu}\ (20^{\circ}C)$.

4. MATHEMATICAL DESCRIPTION

4.1. SUPERPOSITION HYPOTHESIS

In standardizing the recorded data in order to investigate the appliability of the superposition hypothesis in thermal creep analyses of concrete structures, the creep profiles displayed in figs. (1) to (5) are scaled down as if obtained for the reference stress / cold strength ratio $s = 0.2$. The overlapping of curves in figs. (16) and (17) within confidence limits of about $\pm$ 10% justifies the treatment of thermal creep strains as linear thermoviscoelastic strains up to about 300 °C.

4.2. SHAPE OPTIMIZATION

In plotting the creep rate against time in double-logarithmic scale, a linear function of negative slope may be fitted to the scatter of data pairs from each test, as shown in fig. (18)

$$\log\ \varepsilon_{,t} = a\ (s,T) + b\ (s,T)\ \log\ t \qquad (11)$$

Converting to natural logarithm and solving for the real creep increment

$$\varepsilon_{,t} = (2.3025\ a\ (s,T) + b\ (s,T)\ \ln t\ ) \qquad (12)$$

After integration, the function to be fitted reads

$$\varepsilon\ (s,T,t) = \varepsilon\ (s,T,0) + \frac{e^{2.3025\ a\ (s,T)}}{b\ (s,T) + 1}\ t^{\ b\ (s,T) + 1} \qquad (13)$$

Evaluating the diagrams in double-logarithmic scale, the slope becomes

$$b\ (s,T) = \frac{\log \dfrac{\varepsilon_{,t_1}}{\varepsilon_{,t_2}}}{\log \dfrac{t_1}{t_2}} \qquad (14)$$

Whereas the intersecting point on the ordinate is

$$a\ (s,T) = \frac{1}{2}\ (\log\ (\varepsilon_{,t_1}\ .\ \varepsilon_{,t_2})\ -\ b\ (s,T)\ \log\ (t_1\ .\ t_2)\ ) \tag{15}$$

4.3. ANALYSIS OF THERMAL CREEP STRAINS

Consulting figs. (19) and (20), the arithmetical forms of eqs. (14) and (15) become

$$a\ (s,T)\ =\ c\ (s)\ +\ d\ (s)\ T \tag{16}$$

$$b\ (s\ )\ =\ -\ 0.55\ -\ 0.25\ s \tag{17}$$

with

$$c\ (s\ )\ =\ \log\ s\ +\ 0.2$$

$$d\ (s\ )\ =\ 0.0028\ -\ 0.001\ s$$

Substituting eqs. (16) and (17) into eq. (13), the mathematical description of any thermal creep curve is obtainable. The initial strains follow eq. (1) for $T \leq 200\ ^{o}C$ and eq. (2) for $T \leq 200\ ^{o}C$. The duration under load is entered in days; the strains appear in 10^{-4}.

4.4. FORMULA FOR THERMOVISCOELASTIC STRAINS

Using the stress / cold strength ratio $s = 0.2$ as a base, formula (13) may be replaced by another which is limited to the computation of thermoviscoelastic strains. Rewriting eq. (1) as

$$\varepsilon\ (0.2,\ T,\ 0)\ =\ \frac{\sigma\ 0.2}{E\ (20\ ^{o}C)}\ f\ (T) \tag{18}$$

and expressing the applied stress in terms of the strength of concrete as

$$\sigma\ =\ s\ c'_{yu} \tag{19}$$

The author's formula for the obtainment of stress, temperature and time-dependent strains occuring in virgin concrete is arrived at

$$\varepsilon\ (s,T,t)\ =\ s\ \frac{c'_{yu}\ (20\ ^{o}C)}{E\ (20\ ^{o}C)}\ f\ (T)\ +\ \frac{e^{2.3025\ a\ (0.2,\ T)}}{b\ (0.2)\ +\ 1}\ .\ t^{\ b\ (0.2)\ +\ 1} \tag{22}$$

5. NUMERICAL ANALYSIS

5.1. GENERATION OF WEIGHTING FACTORS

A computer program CRELAX first transforms the thermal creep curves as reproduced by formula (22) to sequences of associated relaxation responses on the basis of the creep-relaxation duality as expressed in eq. (34) of the author's paper [3]. Then it regresses the latter to time-dependent relaxation weighting factors by evaluating the history-dependent arithmetical expression [55] of the same paper.

As an example, in fig. (21) the normalized, linear thermoviscoelastic strain curve, experimentally obtained for a test temperature of 300 °C, is compared with that generated by evaluation of formula (22). Also, the corresponding thermal relaxation function and the pertaining relaxation weighting factors are displayed.

5.2. EMPLOYMENT OF WEIGHTING FACTORS

Since for design purposes only the thermal relaxation weighting factors are of interest, these are entered independently in semi logarithmic scale in fig. (22) and table 1. Each profile is really a sequence of discrete time-dependent scalars, since each value is obtained by evaluation of a separate integral. The initial gradients of the relaxation curves - and thus the drop in value of the initial weighting factors - are steeper than those of the creep curves. This observation is satisfying, as it corroborates that the stiffness approach to structural thermoviscoelastic analysis using relaxation weighting factors is more efficient than the flexibility method of approach.

6. MATRIX- THEORETICAL TREATMENT

The stiffness coefficients which link the force and displacement components of a fictitiously subdivided structure, constitute evaluated functions of element geometries and physical properties. In normalizing the relevant creep and relaxation curves, the residual global stiffness matrix of the structure remains untouched by weighting. Owing to their non-dimensional form and rheological nature, the author's thermal relaxation weighting factors may be employed independently even of the structure's geometry and the kind of stiffness method.

Following eq. (59) of the paper mentioned above [3], the step-wise uncoupled load-deformation matrix equation of the transient thermoviscoelastic stress analysis problem may be established for a time instant t_i as

$$G\,(T,\tau,0)\;\underline{W}^{t}\,(t_i)\;\underline{K'}\;\underline{W}\,(t_i)\;G\,(T,\tau,0)\;\underline{u}\,(t_i) =$$

$$G\,(T,\tau,0)\;\underline{W}^{t}\,(t_i)\;\;\underline{R'}\;\underline{\Theta}\,(t_i) + \underline{f'} \qquad (23)$$

where G is the temperature and age-dependent modulus of elasticity, $\underline{W}$ is a column of thermal relaxation weighting factors, $\underline{K'}$ is the residual stiffness matrix, $\underline{u}$ is the displacement vector, $\underline{R'}$ is the residual thermal load vector, $\underline{\Theta}$ is the vector expressing the temperature distribution and $\underline{F'}$ is the residual force vector.

The applicability of thermal relaxation weighting factors in creep analyses has been demonstrated by the author elsewhere [1,3].

7. REFERENCES

(1) Gross, H., "Computer-Aided Thermal Creep Analysis of Concrete Continua", Ph. D. Thesis, London University, Feb. 1973.

(2) Gross, H., "A Testing Machine for Thermal Creep of Concrete", Res. Rep. CSTR 71/6. Rept. of Civ. Eng., Imperial College, London, Sept. 1971.

(3) Gross, H., "Thermoviscoelastic Axisymmetric Stress Analysis by finite Element and finite Difference Computer Techniques", 1st Int. Conf. on SMiRT, Berlin, Sept. 1971.

8. ACKNOWLEDGEMENT

This paper has been extracted from the author's thesis on the project "Computer-aided thermal creep analysis of concrete continua" which was sponsored by the Building Research Station of the Department of the Environment, U.K., and conducted at Imperial College of Science and Technology under the general supervition of Professor A.L.L. Baker and Dr. P.J.E. Sullivan, to whom the author is grateful.

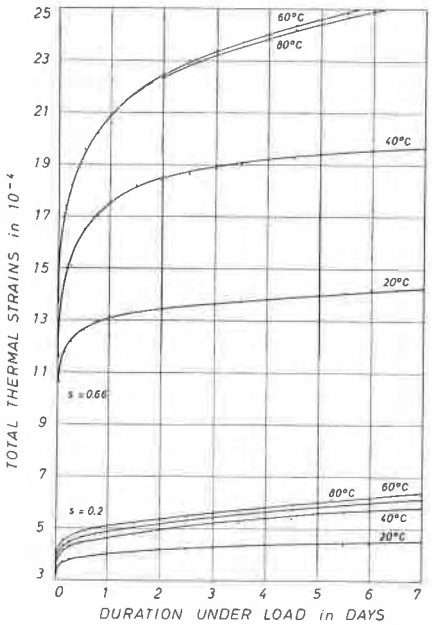

FIG. 1 LOW TEMPERATURE CREEP FOR STRESS / COLD STRENGTH RATIOS OF 0.2 & 0.66

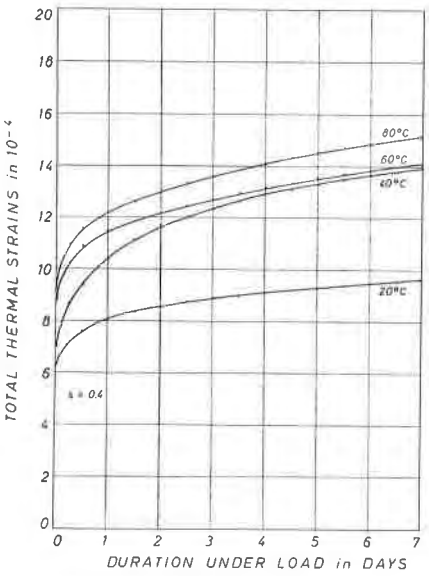

FIG 2 LOW TEMPERATURE CREEP FOR A STRESS / COLD STRENGTH RATIO OF 0.4

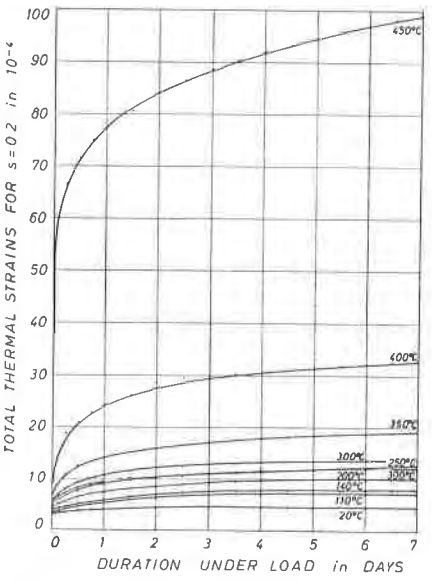

FIG. 3 HIGH TEMPERATURE CREEP FOR A STRESS / COLD STRENGTH RATIO OF 0.2

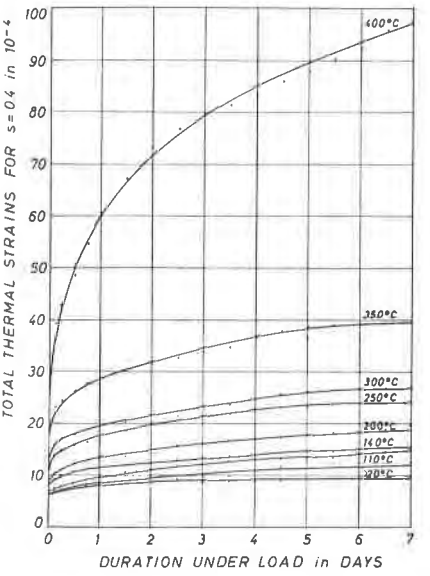

FIG. 4 HIGH TEMPERATURE CREEP FOR A STRESS / COLD STRENGTH RATIO OF 0.4

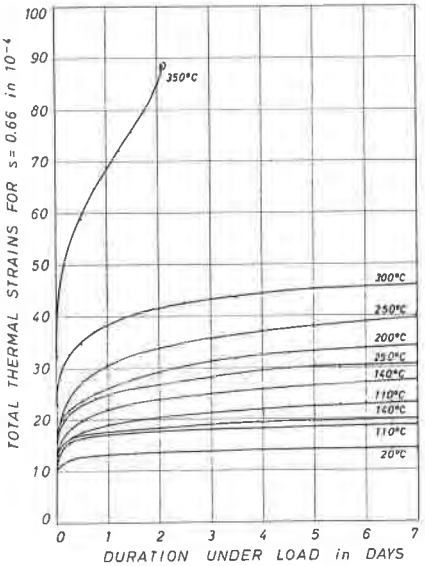

FIG 5 HIGH TEMPERATURE CREEP FOR A STRESS / COLD STRENGTH RATIO OF 0.66

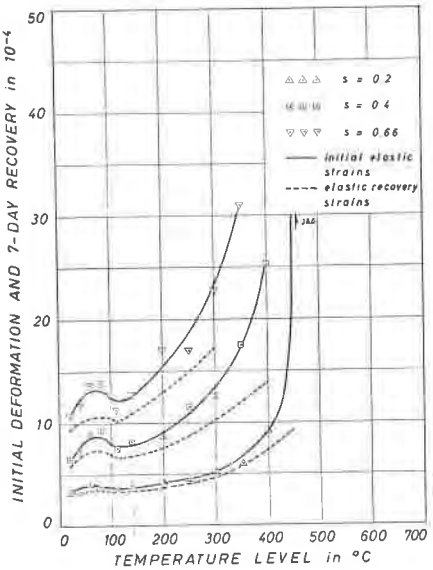

FIG 6 INITIAL & RECOVERED THERMO-ELASTIC STRAINS

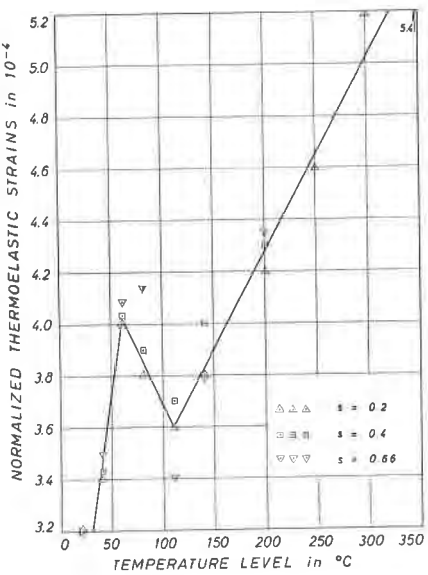

FIG 7 THERMOELASTIC STRAINS NORMALIZED TO A STRESS LEVEL OF 0.2

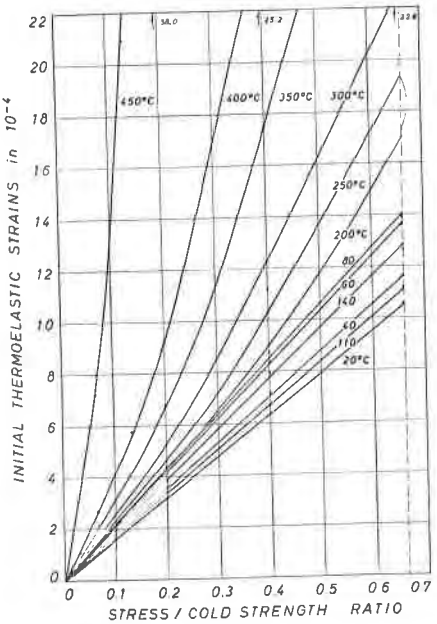

FIG 8 LOAD-DEPENDENT INITIAL THERMOELASTIC STRAINS

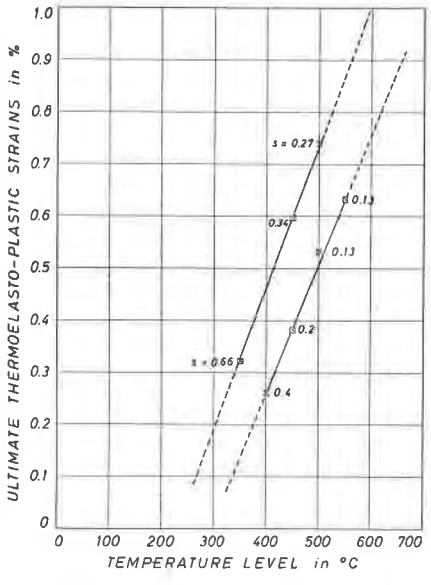

FIG. 9 LIMITS FOR ULTIMATE THERMO-ELASTO-PLASTIC STRAINS

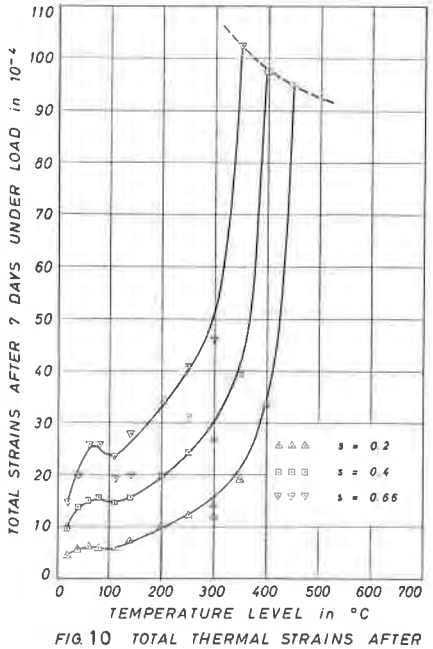

FIG. 10 TOTAL THERMAL STRAINS AFTER SEVEN DAYS UNDER LOAD

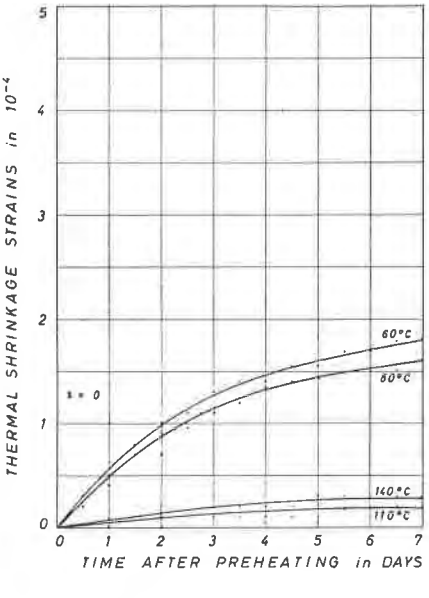

FIG. 11 THERMAL SHRINKAGE

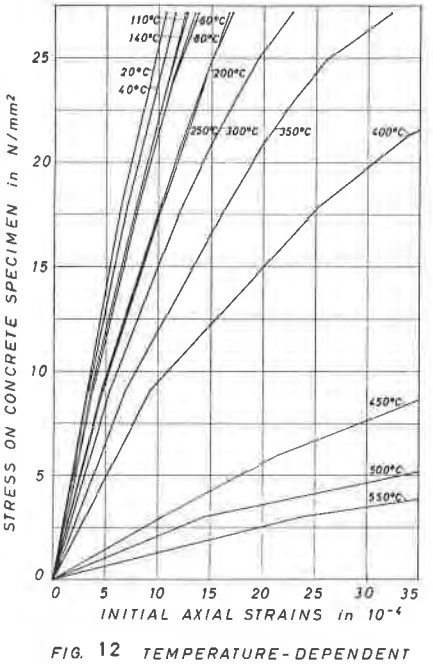

FIG. 12 TEMPERATURE-DEPENDENT STRESS-STRAIN CURVES

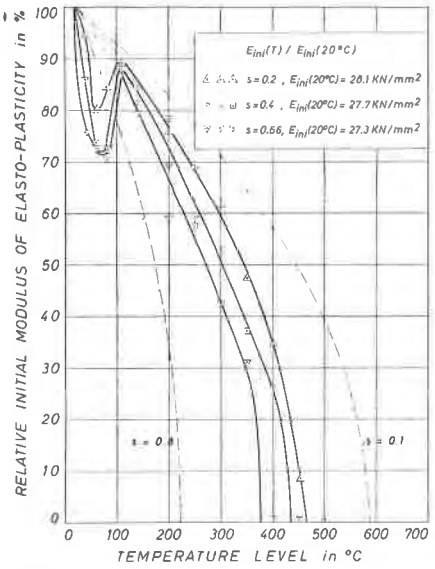

FIG. 13 RELATIVE INITIAL MODULUS OF THERMOELASTO-PLASTICITY

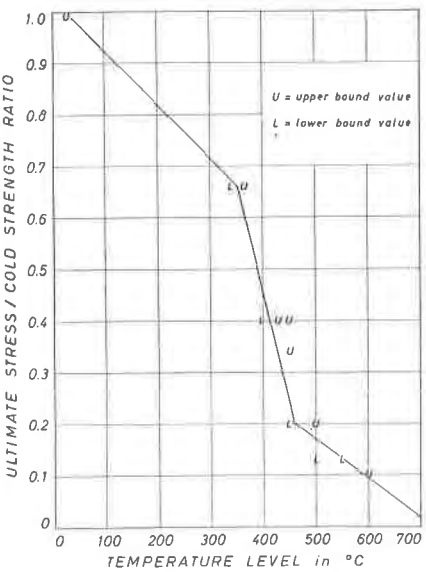

FIG 14 LIMIT FOR ULTIMATE STRESS / COLD STRENGTH RATIO

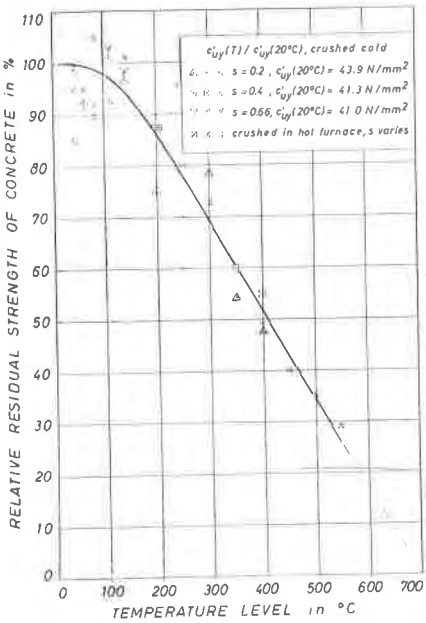

FIG 15 TEMPERATURE-DEPENDENT CYLINDER STRENGTH

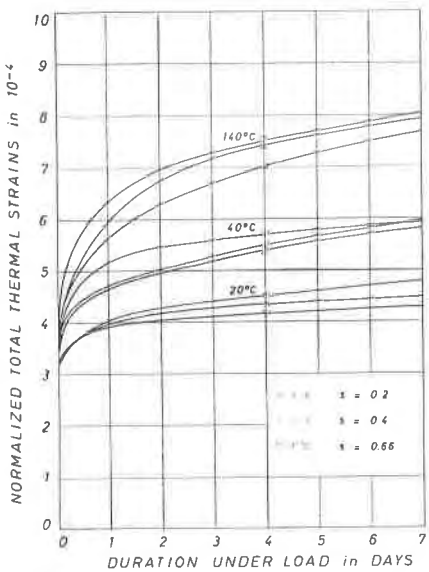

FIG 16 LOW TEMPERATURE CREEP NORMALIZED TO A STRESS LEVEL OF 0.2

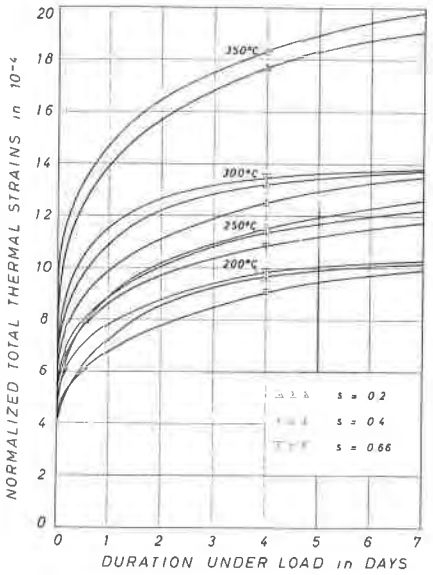

FIG 17 HIGH TEMPERATURE CREEP NORMALIZED TO A STRESS LEVEL OF 0.2

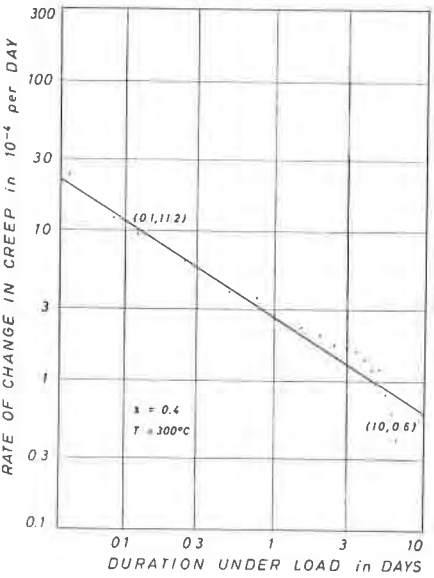

FIG 18 RATE OF CHANGE IN CREEP IN LOG-LOG SCALE

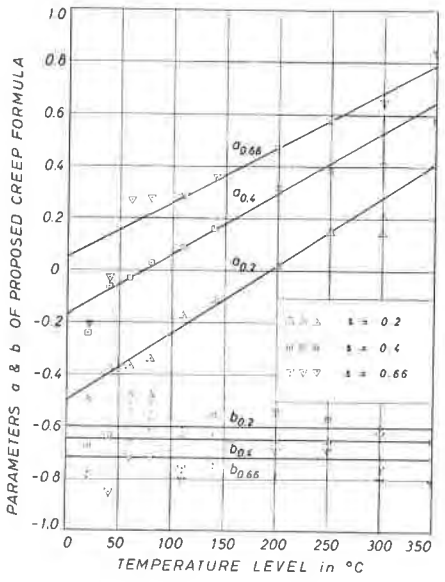

FIG 19 TEMPERATURE-DEPENDENT PARAMETERS OF PROPOSED CREEP FORMULA

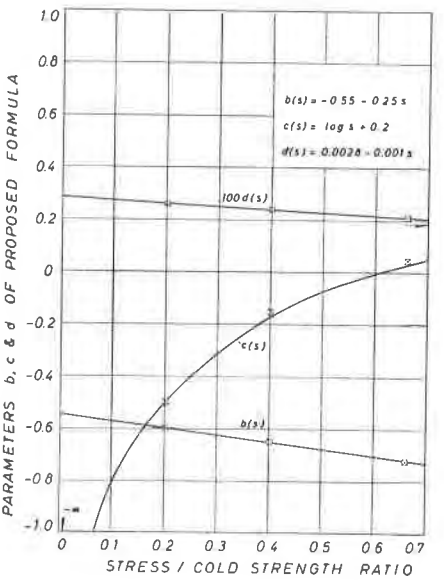

FIG 20 STRESS-DEPENDENT PARAMETERS OF PROPOSED CREEP FORMULA

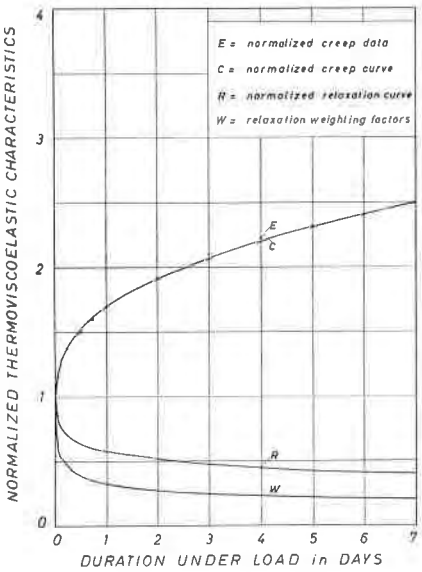

FIG 21 THERMOVISCOELASTIC CHARACTERISTICS OF CONCRETE AT 300°C

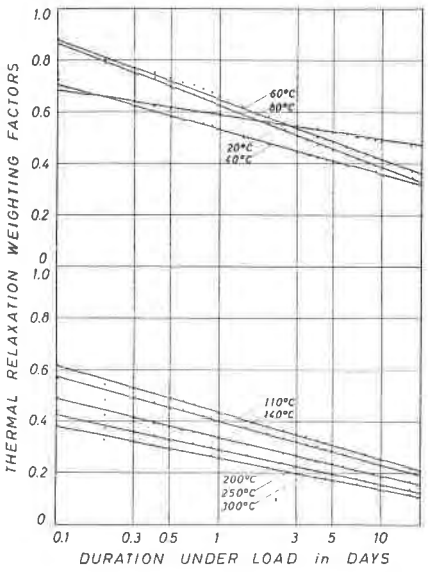

FIG 22 THERMAL RELAXATION WEIGHTING FACTORS IN SEMI-LOG SCALE

Table 1 Normalized thermal relaxation weighting factors

t \ T	20	40	60	80	110	140	200	250	300°C
0 d	1.0	1.0	1.0	1.0	1.0	1.0	1.0	1.0	1.0
0.1	0.68	0.71	0.88	0.86	0.62	0.57	0.49	0.42	0.38
0.2	0.66	0.65	0.81	0.79	0.56	0.52	0.44	0.38	0.34
0.3	0.64	0.62	0.77	0.75	0.53	0.49	0.41	0.36	0.32
0.4	0.63	0.60	0.74	0.72	0.51	0.47	0.39	0.35	0.31
0.5	0.62	0.58	0.72	0.70	0.49	0.45	0.38	0.34	0.30
0.6	0.61	0.57	0.70	0.68	0.48	0.44	0.37	0.33	0.28
0.7	0.60	0.56	0.68	0.67	0.46	0.43	0.36	0.32	0.28
0.8	0.60	0.55	0.67	0.65	0.45	0.42	0.35	0.31	0.27
0.9	0.59	0.54	0.66	0.64	0.44	0.41	0.34	0.30	0.26
1	0.59	0.53	0.65	0.63	0.43	0.40	0.33	0.29	0.26
2	0.56	0.48	0.58	0.55	0.38	0.35	0.29	0.25	0.22
3	0.55	0.45	0.54	0.51	0.35	0.32	0.27	0.23	0.20
4	0.54	0.43	0.51	0.48	0.33	0.30	0.25	0.21	0.18
5	0.52	0.41	0.49	0.46	0.31	0.28	0.23	0.19	0.17
6	0.51	0.39	0.47	0.44	0.30	0.27	0.22	0.19	0.16
7	0.50	0.38	0.45	0.42	0.28	0.26	0.21	0.18	0.15
8	0.50	0.38	0.44	0.40	0.27	0.25	0.20	0.17	0.15
9	0.49	0.37	0.43	0.39	0.26	0.24	0.19	0.16	0.14
10	0.49	0.36	0.42	0.39	0.25	0.23	0.19	0.15	0.13
15	0.48	0.33	0.38	0.34	0.22	0.20	0.16	0.13	0.11